Electronic Supplementary Material (ESI) for Organic & Biomolecular Chemistry.

Supporting information of:

The irony of chirality – Unveiling the distinct mechanistic binding and activities of 1-(3-(4-Amino-5-(7-methoxy-5-methylbenzo[b]thiophen-2-yl)-7H-pyrrolo[2,3-d]pyrimidin-7-yl)pyrrolidin-1-yl)prop-2-en-1-one enantiomers as irreversible covalent FGFR4 inhibitors

Farideh Badichi Akher, Abdolkarim Farrokhzadeh*, Fisayo A. Olotu, Clement Agoni and Mahmoud E.S. Soliman*

Molecular Bio-computation and Drug Design Laboratory, School of Health Sciences, University of KwaZulu-Natal, Westville Campus, Durban 4001, South Africa
*Corresponding Authors: Mahmoud E. Soliman and Abdolkarim Farrokhzadeh

Email: soliman@ukzn.ac.za and farokhzad_amin@yahoo.com
Telephone: +27 (0) 31 260 8048, Fax: +27 (0) 31 260 7872

Figure S1. The 3GQI (FGFR1) and 4TYI (FGFR4) sequence.

Figure S2. Comparative stability of unbound (black), 9**g**- (green) and 9**h**-bound (red) FGFR4 for MD1 **[A]** Whole structure Cα RMSD plot of the three systems **[B]** Post-equilibrated whole-structure Cα RMSD plot from 200-250 ns showing the degree of structural instability at these periods.

Figure S3. Comparative stability of unbound (black), 9**g**- (green) and 9**h**-bound (red) FGFR4 for MD2 **[A]** Whole structure Cα RMSD plot of the three systems **[B]** Post-equilibrated whole-structure Cα RMSD plot from 200-250 ns showing the degree of structural instability at these periods.

Table S1. The finally equilibrated RMSD (FE-RMSD) values for MD1 and MD2.

Table S2. Total binding free energies and energy contributions of 9**g** and 9**h** in complex with FGFR4 (kcal/mol). Replicate results are also shown which include MD1 and MD2 confirming the results are statistically valid.

Table S3. Decomposition of the relative binding free energies (in kcal/mol) for FGFR4-9**h** of MD1.

Table S4. Decomposition of the relative binding free energies (in kcal/mol) for FGFR4-9**h** of MD2.

Table S5. Decomposition of the relative binding free energies (in kcal/mol) for FGFR4-9**g** of MD1.

Table S6. Decomposition of the relative binding free energies (in kcal/mol) for FGFR4-9**g** of MD2.

3GQI.pdb (FGFR1)

```
449 MGHHHHHHMAGVSEYELPEDPRWELPRDRLVLGKPLGEGAFGQVVLAEAI
499 GLDKDKPNRVTKVAVKMLKSDATEKDLSDLISEMEMMKMIGKHKNIINLL
549 GACTQDGPLYVIVEYASKGNLREYLQARRPPGLEFSFNPSHNPEEQLSSK
599 DLVSCAYQVARGMEYLASKKCIHRDLAARNVLVTEDNVMKIADFGLARDI
649 HHIDYYKKTTNGRLPVKWMAPEALFDRIYTHQSDVWSFGVLLWEIFTLGG
699 SPYPGVPVEELFKLLKEGHRMDKPSNCTNELYMMMRDCWHAVPSQRPTFK
749 QLVEDLDRIVALTSNQEYLDLSMPLDR
```

4TYI.pdb (FGFR4)

```
443 AMGSAGLVSLDLPLDPLWEFPRDRLVLGKPLGEGCFGQVVRAEAFGMDPA
493 RPDQASTVAVKMLKDNASDKDLADLVSEMEVMKLIGRHKNIINLLGVCTQ
543 EGPLYVIVECAAKGNLREFLRARRPPGPDLSPDGPRSSEGPLSFPVLVSC
593 AYQVARGMQYLESRKCIHRDLAARNVLVTEDNVMKIADFGLARGVHHIDY
643 YKKTSNGRLPVKWMAPEALFDRVYTHQSDVWSFGILLWEIFTLGGSPYPG
693 IPVEELFSLLREGHRMDRPPHCPPELYGLMRECWHAAPSQRPTFKQLVEA
743 LDKVLLAVSEE
```

Figure S1. The 3GQI (FGFR1) and 4TYI (FGFR4) sequence.

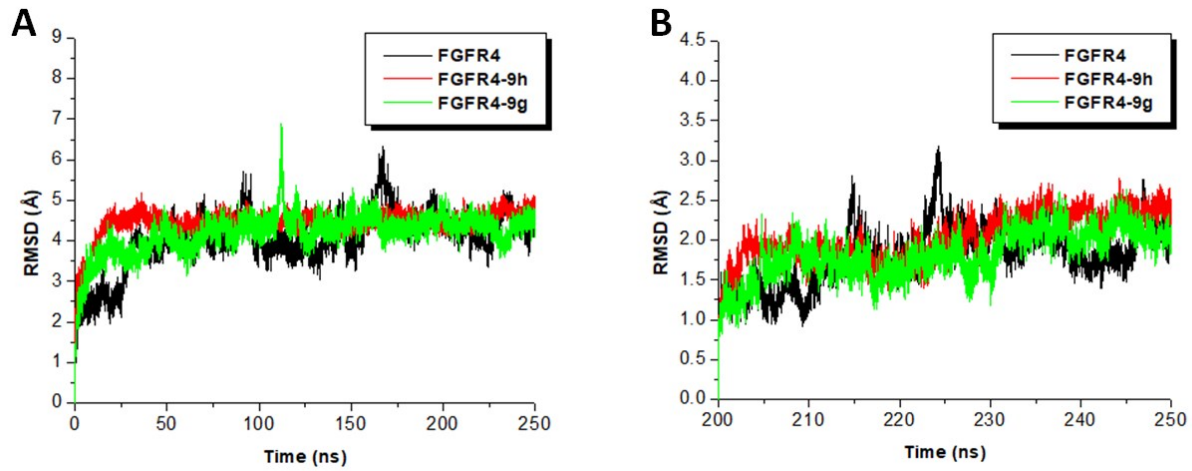

Figure S2. Comparative stability of unbound (black), 9**g**- (green) and 9**h**-bound (red) FGFR4 for MD1 **[A]** Whole structure Cα RMSD plot of the three systems **[B]** Post-equilibrated whole-structure Cα RMSD plot from 200-250 ns showing the degree of structural instability at these periods.

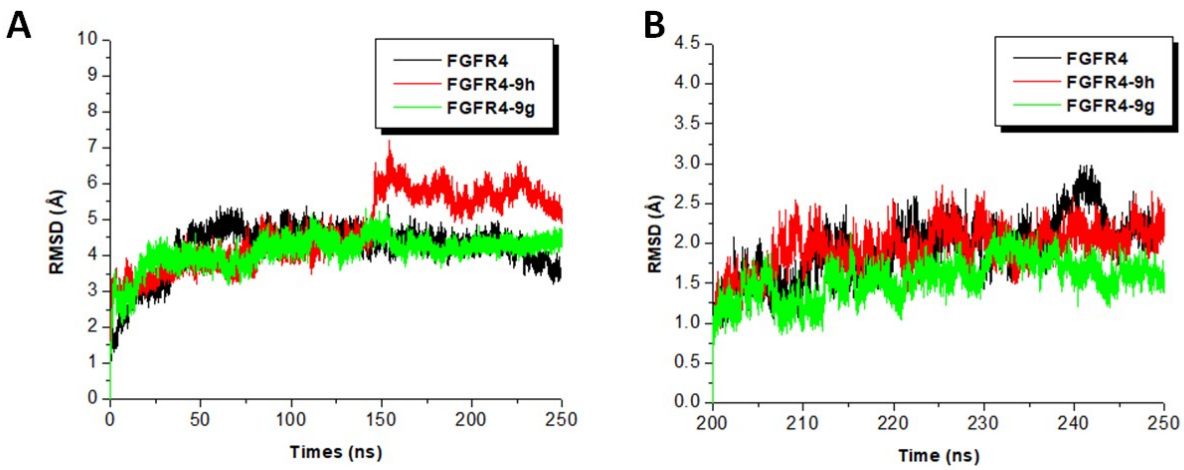

Figure S3. Comparative stability of unbound (black), 9**g**- (green) and 9**h**-bound (red) FGFR4 for MD2 **[A]** Whole structure Cα RMSD plot of the three systems **[B]** Post-equilibrated whole-structure Cα RMSD plot from 200-250 ns showing the degree of structural instability at these periods.

Table S1. The finally equilibrated RMSD (FE-RMSD) values for MD1 and MD2.

	Equilibrated values	FGFR4	FGFR4-9**h**	FGFR4-9**g**
MD1	FE-RMSD (Å)	2.02 (1.92)	1.82 (1.37)	1.82 (1.18)
MD2	FE-RMSD (Å)	2.13 (1.34)	1.93 (1.02)	1.55 (0.83)

The values in parenthesis correspond to the active site residues backbone Cα atoms.

Table S2. Total binding free energies and energy contributions of 9**g** and 9**h** in complex with FGFR4 (kcal/mol). Replicate results are also shown which include MD1 and MD2 confirming the results are statistically valid.

	Complexes			
	9**g**		9**h**	
Energy	MD1	MD2	MD1	MD2
ΔE_{vdW}	-51.84	-51.88	-48.18	-47.76
ΔE_{elel}	-80.88	-82.43	-78.22	-77.69
ΔG_{gas}	-132.57	-134.90	-126.15	-125.45
$\Delta G_{ele,sol(GB)}$	46.26	42.00	43.99	43.35
$\Delta G_{np,sol}$	-7.49	-6.85	-7.76	-8.37
ΔG_{sol}	38.77	35.42	36.23	34.77
ΔG_{bind}	-63.67	-59.16	-47.12	-45.79
IC50	**5.31**		**82.72**	

Table S3. Decomposition of the relative binding free energies (in kcal/mol) for FGFR4-9**h** of MD1.

Residues	Vander Waals	Electrostatic	polar solvation	Non-polar solvation	Total
LEU32	-2.206	-0.3	0.907	-0.327	-1.926
GLY33	-1.787	-1.494	1.503	-0.181	-1.959
GLY38	-1.35	1.278	-0.5	-0.128	-0.7
GLN39	-0.702	0.093	0.005	-0.015	-0.619
VAL40	-1.953	0.029	-0.292	-0.302	-2.518
ALA60	-0.386	-0.191	0.151	-0.029	-0.455
LYS62	-0.614	-3.341	3.247	-0.122	-0.83
MET83	-0.036	-0.024	0.055	-0.004	-0.009
ILE93	-0.418	0.097	-0.066	-0.044	-0.431
VAL109	-0.347	0.086	-0.038	-0.051	-0.35
GLU110	-0.251	0.931	-0.771	-0.019	-0.11
CYS111	-0.462	-0.01	0.505	-0.031	0.002
ALA112	-0.561	-0.162	0.589	-0.063	-0.197
ALA113	-0.122	0.022	0.041	-0.01	-0.069
LYS114	-0.064	-1.693	1.75	0	-0.007
GLY115	-0.238	0.029	0.033	-0.046	-0.222
ASN116	-0.176	-0.203	0.132	-0.007	-0.254
GLU119	-0.032	3.188	-4.115	0	-0.959
ARG170	-0.086	-6.046	6.153	-0.001	0.02
ARG175	-0.116	-5.243	5.469	0	0.11
LEU178	-1.107	0.021	0.073	-0.182	-1.195
ALA188	-0.151	-0.124	0.088	-0.019	-0.206
ASP189	-0.238	5.505	-5.384	-0.038	-0.155
VAL196	-0.041	0.308	-0.284	0	-0.017
HID198	-0.791	-1.344	2.829	-0.204	0.49
ILE199	-0.356	-0.969	1.246	-0.342	-0.421
ASP200	-0.597	7.606	-6.843	-0.038	0.128
TYR201	-2.798	-1.74	2.089	-0.475	-2.924
TYR202	-0.244	0.366	-0.201	-0.004	-0.083
LYS203	-0.122	-5.683	5.886	-0.021	0.06

Table S4. Decomposition of the relative binding free energies (in kcal/mol) for FGFR4-9**h** of MD2.

Residues	Vander Waals	Electrostatic	polar solvation	Non-polar solvation	Total
LEU32	-1.506	-0.112	0.226	-0.27	-1.662
GLY33	-0.321	-0.905	0.293	0	-0.933
GLY38	-1.378	1.847	-0.714	-0.116	-0.361
GLN39	-0.608	-0.42	0.542	-0.004	-0.49
VAL40	-2.003	0.052	-0.32	-0.311	-2.582
ALA60	-0.587	-0.316	0.221	-0.068	-0.75
LYS62	-0.668	-3.786	3.676	-0.144	-0.922
MET83	-0.057	-0.046	0.087	-0.009	-0.025
ILE93	-0.694	0.054	-0.047	-0.054	-0.741
VAL109	-0.462	0.103	-0.082	-0.065	-0.506
GLU110	-0.316	1.102	-0.754	-0.017	0.015
CYS111	-0.644	0.134	0.286	-0.05	-0.274
ALA112	-0.611	-0.075	0.604	-0.062	-0.144
ALA113	-0.109	0.039	0.022	-0.005	-0.053
LYS114	-0.069	-1.94	1.01	0	-0.999
GLY115	-0.28	-0.06	0.182	-0.061	-0.219
ASN116	-0.505	-0.556	0.486	-0.077	-0.652
GLU119	-0.036	2.759	-3.67	0	-0.947
ARG170	-0.16	-6.233	6.153	-0.036	-0.276
ARG175	-0.632	-5.085	5.099	-0.155	-0.773
LEU178	-1.859	-0.053	0.188	-0.302	-2.026
ALA188	-0.354	-0.093	0.024	-0.053	-0.476
ASP189	-0.645	4.65	-4.595	-0.132	-0.722
VAL196	-0.028	0.174	-0.116	0	0.03
HID198	-0.275	-0.687	1.292	-0.121	0.209
ILE199	-0.458	-0.168	0.566	-0.092	-0.152
ASP200	-0.708	8.635	-8.907	-0.007	-0.987
TYR201	-2.613	-0.47	1.486	-0.391	-1.988
TYR202	-0.966	0.065	0.832	-0.168	-0.237
LYS203	-0.401	-6.278	6.4	-0.013	-0.292

Table S5. Decomposition of the relative binding free energies (in kcal/mol) for FGFR4-9**g** of MD1.

Residues	Vander Waals	Electrostatic	polar solvation	Non-polar solvation	Total
LEU32	-1.21	-1.273	0.476	-0.198	-2.205
GLY33	-1.639	-0.753	0.964	-0.32	-1.748
GLY38	-1.065	-0.416	0.918	-0.092	-0.655
GLN39	-1.014	-0.57	0.588	-0.034	-1.03
VAL40	-0.577	0.065	0.026	-0.108	-0.594
ALA60	-0.035	0.028	-0.005	-0.004	-0.016
LYS62	-0.424	-3.908	2.557	-0.055	-1.83
MET83	-0.012	0.001	0.015	0	0.004
ILE93	-0.045	0.012	0.012	0	-0.021
VAL109	-0.023	-0.009	0.014	0	-0.018
GLU110	-0.018	-0.419	0.434	0	-0.003
CYS111	-0.037	0.039	0.016	-0.001	0.017
ALA112	-0.147	-0.06	0.184	-0.021	-0.044
ALA113	-0.04	-0.045	0.097	-0.001	0.011
LYS114	-0.079	0.447	-0.345	-0.001	0.022
GLY115	-0.507	-0.325	0.367	-0.114	-0.579
ASN116	-0.9472	-1.629	1.875	-0.266	-0.9672
GLU119	-0.535	-2.587	2.781	-0.149	-0.49
ARG170	-0.009	0.543	-0.512	0	0.022
ARG175	-0.859	0.978	1.117	-0.444	0.792
LEU178	-0.867	-0.054	0.165	-0.173	-0.929
ALA188	-0.11	-0.086	0.002	0	-0.194
ASP189	-1.02	-2.057	5.476	-0.139	2.26
VAL196	-0.101	-0.098	0.13	-0.004	-0.073
HID198	-1.654	-0.87	2.087	-0.132	-0.569
ILE199	-1.67	0.192	0.162	-0.124	-1.44
ASP200	-3.619	-0.809	0.94	0	-3.488
TYR201	-1.279	0.016	0.076	0	-1.187
TYR202	-1.309	-0.088	0.271	-0.035	-1.161
LYS203	-0.066	0.325	-0.24	-0.002	0.017

Table S6. Decomposition of the relative binding free energies (in kcal/mol) for FGFR4-9**g** of MD2.

Residues	Vander Waals	Electrostatic	polar solvation	Non-polar solvation	Total
LEU32	-2.024	-1.68	0.032	0	-3.672
GLY33	-1.193	0.012	0.091	-0.018	-1.108
GLY38	-1.423	0.546	0.153	-0.121	-0.845
GLN39	-0.486	0.077	0.033	-0.018	-0.394
VAL40	-0.8765	0.011	-0.017	-0.054	-0.9365
ALA60	-0.004	0.018	-0.008	0	0.006
LYS62	-0.339	2.159	-1.536	-0.131	0.153
MET83	-0.006	0.02	-0.007	0	0.007
ILE93	-0.004	-0.006	0.015	0	0.005
VAL109	-0.006	0.022	-0.018	0	-0.002
GLU110	-0.002	-0.64	0.638	0	-0.004
CYS111	-0.002	-0.017	0.028	0	0.009
ALA112	-0.001	-0.019	0.026	0	0.006
ALA113	-0.001	0	0.003	0	0.002
LYS114	-0.001	0.396	-0.39	0	0.005
GLY115	-0.001	0.016	-0.009	0	0.006
ASN116	-0.005	0.053	-0.031	0	0.017
GLU119	-0.002	-0.419	0.426	0	0.005
ARG170	-0.573	-2.532	1.423	-0.082	-1.764
ARG175	-0.038	0.493	-0.376	-0.444	-0.365
LEU178	-0.007	0.016	-0.012	-0.273	-0.276
ALA188	-0.009	0.046	-0.05	0	-0.013
ASP189	-0.089	-1.651	1.901	-0.004	0.157
VAL196	-0.195	-0.258	0.354	-0.01	-0.109
HID198	-4.262	-2.408	4.459	-0.568	-2.779
ILE199	-1.939	-0.726	0.515	-0.043	-2.193
ASP200	-3.02	-2.244	4.01	-0.275	-1.529
TYR201	-0.283	-0.17	0.226	-0.002	-0.229
TYR202	-5.125	-0.66	1.921	-0.567	-4.431
LYS203	-0.488	0.753	-0.399	-0.008	-0.142